Available online at www.sciencedirect.com

ScienceDirect

Energy Procedia 114 (2017) 3282 – 3290

Energy Procedia

13th International Conference on Greenhouse Gas Control Technologies, GHGT-13, 14-18 November 2016, Lausanne, Switzerland

Potential for Fault Reactivation due to CO_2 Injection in a Semi-Closed Saline Aquifer

Victor Vilarrasa[a,b]*, Roman Y. Makhnenko[a,c], Lyesse Laloui[a]

[a]*Laboratory of Soil Mechanics, École Polytechnique Fédérale de Lausanne, EPFL ENAC IIC LMS, GC – Station 18, 1015 Lausanne, Switzerland*

[b]*Institute of Environmental Assessment and Water Research, Spanish National Research Council (IDAEA-CSIC), Jordi Girona 18-26, 08034 Barcelona, Spain*

[c]*Department of Civil & Environmental Engineering, University of Illinois at Urbana-Champaign, 205 North Mathews Ave, Urbana, IL, 61801-2352, USA*

Abstract

CO_2 injection in extensive saline aquifers that present no faults is unlikely to damage the caprock sealing capacity. In contrast, CO_2 injection in closed reservoirs will induce a large pressure buildup that may reactivate the low-permeable faults that bound the reservoir. However, the vast majority of CO_2 storage formations will be extensive saline aquifers bounded by a limited number of low-permeable faults. Such storage formations have received little attention and are the focus of this study. We model an extensive aquifer bounded by a heterogeneous low-permeable fault on one side and having open boundaries on the other sides. Simulation results show that the storage formation pressurizes between the injection well and the low-permeable fault, causing total stress changes and effective stress reduction around the fault. These changes lead to yielding of the fault core that is next to the lower half of the storage formation when injecting in the hanging wall. The yield of the fault core would induce a sequence of microseismic events with accumulated seismic moment equivalent to an earthquake of magnitude 1.7, which would not be felt on the ground surface and would not enhance permeability of the ductile clay-rich fault.

Peer-review under responsibility of the organizing committee of GHGT-13.

Keywords: geomechanics; induced seismicity; overpressure; hydro-mechanical coupling

* Corresponding author. Tel.: +34-93-400-6100; fax: +34-93-204-5904.
E-mail address: victor.vilarrasa@upc.edu

Peer-review under responsibility of the organizing committee of GHGT-13.
doi:10.1016/j.egypro.2017.03.1460

1. Introduction

Large volumes of carbon dioxide (CO_2) will be injected in deep saline aquifers to mitigate climate change, inducing pressure buildup that may lead to fault reactivation. Failure conditions are unlikely to be reached in extensive aquifers [1]. As a result, the caprock sealing capacity will be maintained and CO_2 leakage across the caprock is improbable. However, in closed aquifers, overpressure will rapidly increase once the pressure perturbation cone reaches low-permeable boundaries of the aquifer [2, 3]. Thus, failure conditions may eventually be met in the low-permeable faults that bound aquifers. Fault reactivation may induce seismic events [4, 5], which could be potentially felt at the ground surface [6] and cause public opposition that may end up with the closure of CO_2 storage projects, as already occurred after the induced earthquakes in a geothermal project at Basel, Switzerland [7]. Thus, fault reactivation that could lead to felt induced seismicity should be avoided to achieve a successful deployment of CO_2 storage projects.

The vast majority of suitable storage formations will neither be extensive aquifers nor closed aquifers, but will correspond to relatively extensive aquifers bounded by a limited number of low-permeable faults [8-10]. However, this kind of aquifers has received limited attention and needs further consideration. The numerical models used for studying fault reactivation usually represent closed aquifers in which CO_2 injection induces a high overpressure [e.g., 11, 12]. Such models may be representative of compartmentalized reservoirs [13, 14], which can rapidly reach their storage capacity due to overpressure limitations [15, 16]. Nevertheless, in the presence of a limited number of low-permeable barriers or if the permeability across faults is relatively high, pressure builds up at a lower rate [17], and thus, fault reactivation may not be an issue.

In this study, we model an extensive aquifer bounded by a low-permeable fault on one side and having open boundaries on the other sides. First, we present the geometry and material properties of the considered model. Then, we analyze the effect of fault permeability on the potential of fault reactivation and discuss the implications for geologic carbon storage projects. Finally, we draw the conclusions of this study.

2. Methods

A schematic representation of the numerical model, which includes a fault on one side of the injection well, is shown in Fig. 1. On the other side of the well, the model extends laterally for 20 km, so that the boundary does not have any effect on the evolution of overpressure for the considered duration of CO_2 injection. The fault has an offset of 25 m and the aquifer has a thickness of 50 m. Therefore, half of the aquifer is still connected except for the presence of the fault. CO_2 is injected with a constant mass flow rate through a horizontal well on the hanging wall of the fault. The model is a 2D cross section, with plane strain symmetry given by the horizontal injection well, which injects $2.0 \cdot 10^{-3}$ kg/s of CO_2 per meter normal to the model during half a year. Initial pore pressure is hydrostatic and equal to 15 MPa at the top of the reservoir, which is placed at 1.5 km deep. The stress state corresponds to a normal faulting stress regime, in which the vertical stress has a gradient of 23 MPa/km and the horizontal stresses are 70 % of the vertical stress. The fault dips 60º, so it is critically oriented in normal faulting stress regimes [18].

We solve this hydro-mechanical problem using the fully coupled finite element code CODE_BRIGHT [19, 20], extended for CO_2 injection [21, 22]. To simulate CO_2 injection, mass and momentum conservation of each phase, i.e., CO_2 and brine, have to be solved. Momentum conservation in porous media is given by Darcy's law. Mass conservation of these two fluids is given by [23],

$$\frac{\partial(\varphi S_\alpha \rho_\alpha)}{\partial t} + \nabla \cdot (\rho_\alpha \mathbf{q}_\alpha) = 0, \qquad \alpha = c, w, \tag{1}$$

where φ [$L^3\ L^{-3}$] is porosity, S_α [–] is saturation of α-phase, ρ_α [$M\ L^{-3}$] is density of α-phase, t [T] is time, and $\mathbf{q}_\alpha$ [$L^3\ L^{-2}\ T^{-1}$] is the volumetric flux of α-phase. To account for the hydro-mechanical coupling, the momentum balance of the solid phase is solved simultaneously. If inertial terms are neglected, the momentum balance reduces to the equilibrium of stresses

$$\nabla \cdot \boldsymbol{\sigma} + \mathbf{b} = \mathbf{0}, \quad (2)$$

where $\boldsymbol{\sigma}$ [M L^{-1} T^{-2}] is the stress tensor and $\mathbf{b}$ [M L^{-2} T^{-2}] is the body forces vector. To assess the potential for fault reactivation, an elasto-plastic behavior of the geomaterials given by the Drucker-Prager yield function is adopted (see [24] for details).

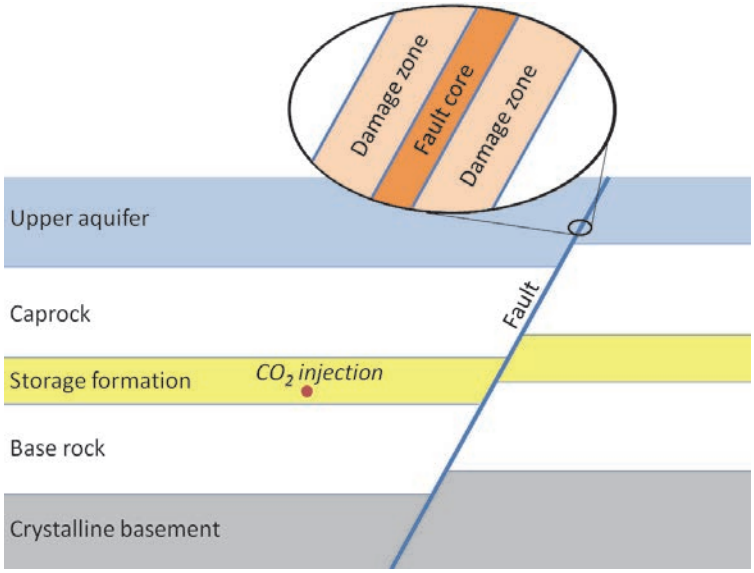

Fig 1. Schematic representation of the model for evaluating the potential of fault reactivation in a semi-closed storage formation.

3. Materials

The aquifer in which CO_2 is injected corresponds to Berea sandstone formation, the caprock and baserock are shales (Opalinus clay), the upper aquifer is the Indiana limestone formation, and the basement is made of Charcoal granite. Tables 1 and 2 include the hydraulic and geomechanical properties for the different rock types and fault, respectively, which have been measured in laboratory experiments at the EPFL or elsewhere [e.g., 25, 26]. Failure properties of shale and granite were adopted from the literature [27, 28], as well as the elastic properties of the granite [29]. CO_2 will flow relatively easy in the storage formation due to its high permeability and low entry pressure. On the other hand, the low permeability and high entry pressure of shale [30] will confine CO_2 in the storage formation and prevent CO_2 leakage through the caprock. The reported values of porosity for the confining layers, crystalline basement, and the fault core are the effective porosities, i.e., those that contribute to flow. Relative CO_2 and water permeabilities are taken as power functions of saturation, with a power of three for the sandstone and the limestone and six for the shale and the granite [31]. Low-permeability (~ 10^{-20} m^2) and relatively low (~ GPa) elastic moduli of caprock and baserock provide characteristic diffusion time for these formations to be ~ 10^9 sec (tens of years), and hence the undrained elastic properties of shale were considered.

The fault is composed by a fault core and a damage zone on both sides of the core (Figure 1). Both the geomechanical and hydraulic properties of the damage zone are different for the sections of the fault that cross clay-rich geomaterials, like the caprock, and siliciclastic or carbonate rocks, like aquifers [32, 33]. Including fault heterogeneity in the hydraulic properties hinders fluid migration if shear slip occurs in the fault [34]. Fault core is made of reconstituted shale, which properties along with the properties of other damaged materials were measured in the laboratory. These characteristics may vary depending on level of damage and applied effective stress. The friction angle of siliciclastic and carbonate rocks, i.e., aquifers, is high, above 30º, but it is low (< 30 º) for clay-rich materials, such as caprock and fault core [29, 30]. Thus, the aquifers are far from being critically stressed, but the

clay-rich materials are close to shear failure conditions. Additionally, failure properties of the sandstone and the limestone were found to be intermediate stress-dependent [25, 35], though is not taken into account in the model. With the assumptions of purely drained (for the storage formation, upper aquifer, basement, fault core, and damage zones) or undrained (caprock and baserock) behavior, linear failure properties independent of intermediate stress, and power law type dependence of water and CO_2 permeabilities from the degree of saturation, the introduced model is assumed to be the first order approach to the problem of CO_2 injection in semi-closed aquifers.

Table 1. Hydraulic properties of the geomaterials included in the model.

Formation	Permeability, k (m^2)	Relative water permeability, k_{rw} (-)	Relative CO_2 permeability, k_{rc} (-)	Gas entry pressure, p_0 (MPa)	van Genuchten shape parameter m (-)	Porosity, φ (-)
Storage formation	$4 \cdot 10^{-14}$	S_w^3	S_c^3	0.02	0.8	0.23
Caprock	$8 \cdot 10^{-20}$	S_w^6	S_c^6	1.5	0.3	0.05
Base rock	$5 \cdot 10^{-20}$	S_w^6	S_c^6	1.5	0.3	0.05
Upper aquifer	$1 \cdot 10^{-14}$	S_w^3	S_c^3	0.20	0.8	0.13
Crystalline basement	$4 \cdot 10^{-20}$	S_w^6	S_c^6	12.0	0.3	0.01
Fault core	$1 \cdot 10^{-19}$	S_w^6	S_c^6	4.0	0.3	0.10
Damage zone reservoirs	$2 \cdot 10^{-13}$	S_w^3	S_c^3	0.02	0.8	0.25
Damage zone confinement layers	$1.5 \cdot 10^{-19}$	S_w^6	S_c^6	5.0	0.3	0.09
Damage zone basement	$1 \cdot 10^{-16}$	S_w^4	S_c^4	1.0	0.5	0.07

Table 2. Geomechanical properties of the geomaterials included in the model.

Formation	Young's modulus, E (GPa)	Poisson ratio, ν(-)	Cohesion, c' (MPa)	Friction angle, ϕ (°)
Storage formation	14.0	0.31	9	42
Caprock	2.8	0.40	6	24
Base rock	3.0	0.39	6	24
Upper aquifer	28.0	0.21	12	31
Crystalline basement	55.0	0.18	60	30
Fault core	1.0	0.30	0	24
Damage zone reservoirs	7.0	0.35	0	30
Damage zone confinement layers	1.4	0.42	0	24
Damage zone basement	42.0	0.30	0	30

4. Results

CO_2 injection in the presence of a low-permeable fault causes an additional pressurization of the aquifer in the region comprised between the well and the fault (Fig. 2a). However, on the other side of the injection well, the resident brine can migrate away from it without finding any flow barrier. This flow pattern leads to pressurization near the fault that is slower than the one that would occur in a closed aquifer. Nevertheless, fluid pressure tends to increase, and thus, failure conditions at the fault may be reached if the injection flow rate is maintained constant. Overpressure causes a decrease of the effective stresses, but also induces changes in the total stresses around the fault that may compromise fault stability (Fig. 2b-2d).

In our model, the onset of plastic strain (or yield that is taken here as a failure point for clay-rich fault) occurs after 40 days of injection. Plastic strain accumulates with time, mainly within the fault core coinciding with the lower half of the storage formation, as shown in Fig. 2e. The length of the fault core that undergoes plastic strain is of 20 m, with a magnitude close to 1%, which yields a mean slip of 0.15 m. The seismic moment can be estimated as the product of the shear modulus of the fault core, the mean slip, and the rupture area. Once the seismic moment is known, the magnitude of the induced earthquake can be calculated using the relationship proposed by Kanamori and Anderson [36]

$$M = \log_{10} \frac{M_0}{1.5} - 10.73, \tag{3}$$

where $M_0 = GAd$ is the seismic moment, G is the shear modulus, A is the rupture area, and d is the mean slip. Assuming that the rupture of the fault extends over the whole length of the injection well and a 2 km long horizontal well, the resulting magnitude of the simulated induced earthquake is 1.7. Since the magnitude is lower than 2, such event would not be felt on the surface and thus, it would be considered as a microseismic event. Such magnitude is similar to the maximum magnitude of the microseismic events that were recorded at In Salah storage site [37].

Figure 3 shows the stress path for the fault core material in deviatoric stress – mean effective stress diagram. Initially, the stress state is close to the yield surface. As overpressure increases due to CO_2 injection, the mean effective stress is reduced, approaching the yield surface. At certain moment (40 days of injection), the stress state touches the yield surface (Fig. 4) and plastic strain starts to develop. Within the framework of the considered model, fluid pressure continues to build up, decreasing the mean effective stress further, but the deviatoric stress evolves by maintaining the stress state on the yield surface (Fig. 3).

5. Discussion

One of the main issues related to geologic carbon storage is felt induced seismicity caused by fault reactivation. On the one hand, fault reactivation may enhance fault permeability and open up migration paths that may lead to CO_2 leakage [5]. However, the hydraulic properties of faults in the reservoir-caprock sequences where CO_2 is planned to be stored are highly heterogeneous, which significantly hinders upward CO_2 flow due to the presence of materials with high gas entry pressure [34]. On the other hand, felt seismic events may cause public opposition that may end up with the closure of CO_2 storage projects, as already occurred with a geothermal project at Basel in which several induced earthquakes were felt by the local population [7].

The earthquake that would be induced with the accumulated plastic strain simulated in our model (magnitude 1.7) is not enough to be felt on the surface. Furthermore, rather than a single event, the fault would likely rupture in a sequence of multiple microseismic events. Thus, the simulated fault reactivation would not cause any nuisances to the local population. Additionally, with on-site microseismic monitoring, correction measures on the flow rate could have been applied to halt fault reactivation.

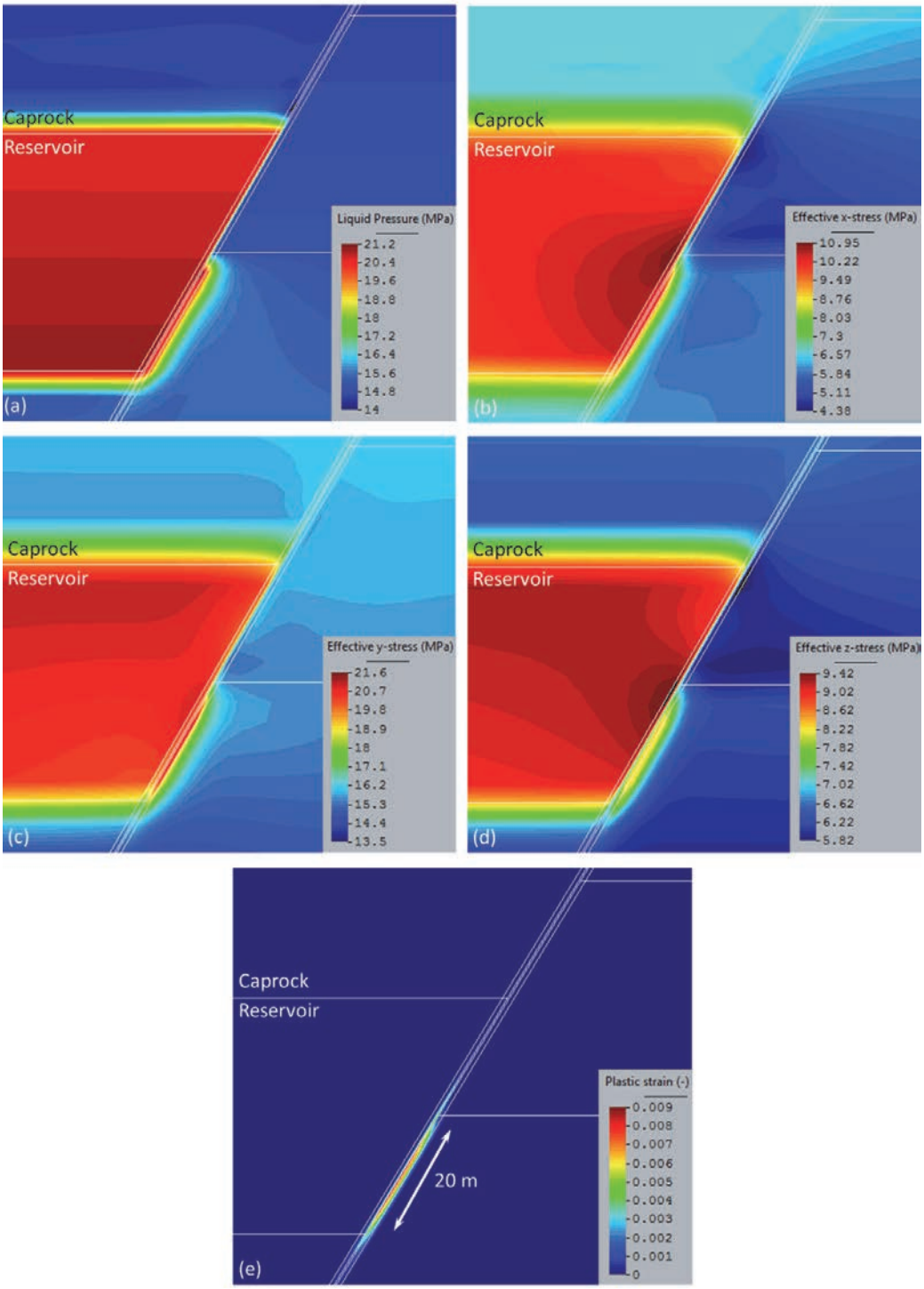

Fig 2. (a) Liquid pressure, (b) effective maximum horizontal stress (in-plane direction), (c) effective vertical stress, (d) effective minimum horizontal stress (out-of-plane direction) and (e) plastic strain after half a year of CO_2 injection.

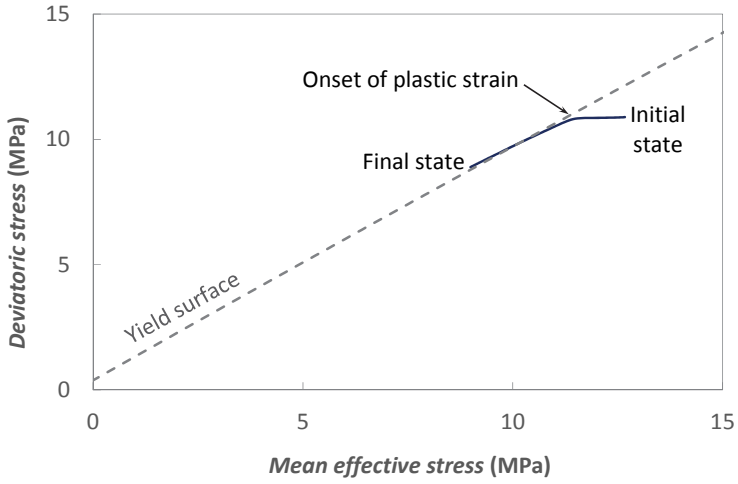

Fig 3. Deviatoric stress versus mean effective stress trajectory of the fault core during half a year of CO_2 injection.

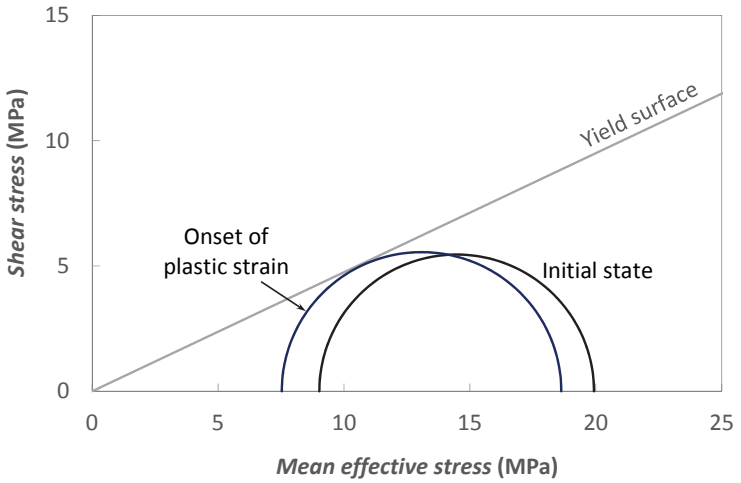

Fig 4. Mohr circles at the fault core prior to injection and at the onset of plastic strain due to CO_2 injection.

Our model includes the heterogeneity that is expected in faults that cross reservoir-caprock sequences in sedimentary basins. We consider a clay-rich fault core and a damage zone on both sides of the fault core and these damage zones are different for each layer. We have based the material properties on laboratory measurements of rocks representative of each geomaterial included in the numerical model. Still, the values of some of the properties that we have used in our model may vary significantly with the stress state and rock type. In particular, fault permeability may differ by several orders of magnitude depending on its structure, i.e., if the fault is a conduit instead of a flow barrier [38].

Another key aspect of induced seismicity is how friction coefficient of the fault evolves once shear failure conditions are reached. In our model, failure conditions do not propagate along the fault inducing a large earthquake, as could be the case if a strain-softening model is implemented [39]. Such kind of behavior may occur in brittle materials, but it is unlikely in faults with a high clay content due to their ductility. In particular, faults with high clay content may accumulate plastic strain aseismically [40], avoiding the brittle behavior that may trigger large

magnitude seismic events. Further investigation on the behavior of clay rich faults is required to reduce the existing uncertainties on the response of faults to CO_2 injection.

Previous studies on fault reactivation considered CO_2 injection into a closed reservoir [e.g., 4, 6, 11]. We model a semi-closed reservoir, which is bounded only on one side. Even though pressure buildup is slower than in a closed reservoir, simulation results suggest that shear failure conditions will eventually be reached on the fault if the injection rate is maintained constant. Since low-permeable faults are expected to be present in extensive saline aquifers, a good characterization to map existing faults and a proper monitoring during CO_2 injection are needed to minimize the risk of fault reactivation that may lead to felt induced seismicity.

6. Conclusions

We model CO_2 injection in a semi-closed aquifer bounded by a low-permeable fault. We include heterogeneity in the structure of the fault, accounting for a fault core and a damage zone on both sides of the core that have different material properties depending on the rock layer they are in contact with, i.e., reservoirs, confining layers, or crystalline basement. Though there is not an excessive overpressure on the side of the storage formation where there is no fault because the resident brine can easily migrate away from the injection well, the low-permeability of the fault induces pressurization of the storage formation between the well and the fault. This pressurization causes total stress changes around the fault and reduces the effective stresses, leading to yield conditions in the fault core. Simulation results show that, when injecting in the hanging wall of the fault, plastic strain accumulates along 20 m in the fault core, coinciding with the lower half of the storage formation in the hanging wall. This plastic strain would cause a sequence of microseismic events with a cumulative moment magnitude equivalent to an earthquake of magnitude 1.7. Such low magnitude would not be felt at the ground surface and, according to laboratory experiments, would not enhance permeability of the ductile clay-rich fault.

Acknowledgements

V.V. acknowledges support from the ‘EPFL Fellows’ fellowship programme co-funded by Marie Curie, FP7 Grant agreement no. 291771. R.M. activities are sponsored by SCCER-SoE (Switzerland) grant KTI.2013.288 and Swiss Federal Office of Energy (SFOE) project CAPROCK #810008154.

References

[1] Vilarrasa, V, Carrera J. Geologic carbon storage is unlikely to trigger large earthquakes and reactivate faults through which CO_2 could leak. Proceedings of the National Academy of Sciences 2015; 112(19):5938-43.

[2] Zhou Q, Birkholzer JT, Tsang CF, Rutqvist J. A method for quick assessment of CO_2 storage capacity in closed and semi-closed saline formations. International Journal of Greenhouse Gas Control 2008; 2(4):626-39.

[3] Mathias SA, de Miguel GJGM, Thatcher KE, Zimmerman RW. Pressure buildup during CO_2 injection into a closed brine aquifer. Transport in Porous Media 2011; 89(3):383-97.

[4] Cappa F, Rutqvist J. Impact of CO_2 geological sequestration on the nucleation of earthquakes. Geophysical Research Letters 2011; 38(17), L17313, doi:10.1029/2011GL048487.

[5] Rinaldi AP, Vilarrasa V, Rutqvist J, Cappa F. Fault reactivation during CO_2 sequestration: Effects of well orientation on seismicity and leakage. Greenhouse Gases: Science and Technology 2015; 5(5):645-56.

[6] Cappa F, Rutqvist J. Seismic rupture and ground accelerations induced by CO_2 injection in the shallow crust. Geophysical Journal International 2012; 190(3):1784-9.

[7] Häring MO, Schanz U, Ladner F, Dyer BC. Characterisation of the Basel 1 enhanced geothermal system. Geothermics 2008; 37(5):469-95.

[8] Hitchon B, Gunter WD, Gentzis T, Bailey RT. Sedimentary basins and greenhouse gases: a serendipitous association. Energy Conversion and Management 1999; 40(8):825-43.

[9] Bachu S. Screening and ranking of sedimentary basins for sequestration of CO_2 in geological media in response to climate change. Environmental Geology 2003; 44(3):277-89.

[10] Verdon JP, Kendall JM, Stork AL, Chadwick RA, White DJ, Bissell RC. Comparison of geomechanical deformation induced by megatonne-scale CO_2 storage at Sleipner, Weyburn, and In Salah. Proceedings of the National Academy of Sciences 2013; 110(30):E2762-71.

[11] Cappa F, Rutqvist J. Modeling of coupled deformation and permeability evolution during fault reactivation induced by deep underground injection of CO_2. International Journal of Greenhouse Gas Control 2011; 5(2):336-46.

[12] Mazzoldi A, Rinaldi AP, Borgia A, Rutqvist J. Induced seismicity within geological carbon sequestration projects: maximum earthquake magnitude and leakage potential from undetected faults. International Journal of Greenhouse Gas Control 2012; 10:434-42.
[13] Vidal-Gilbert S, Tenthorey E, Dewhurst D, Ennis-King J, Van Ruth P, Hillis R. Geomechanical analysis of the Naylor Field, Otway Basin, Australia: Implications for CO_2 injection and storage. International Journal of Greenhouse Gas Control 2010; 4(5):827-39.
[14] Castelletto N, Gambolati G, Teatini P. Geological CO_2 sequestration in multi-compartment reservoirs: Geomechanical challenges. Journal of Geophysical Research: Solid Earth 2013; 118(5):2417-28.
[15] Szulczewski ML, MacMinn CW, Herzog HJ, Juanes R. Lifetime of carbon capture and storage as a climate-change mitigation technology. Proceedings of the National Academy of Sciences 2012; 109(14):5185-9.
[16] Hansen O, Gilding D, Nazarian B, Osdal B, Ringrose P, Kristoffersen JB, Eiken O, Hansen H. Snøhvit: the history of injecting and storing 1 Mt CO_2 in the Fluvial Tubåen Fm. Energy Procedia 2013; 37:3565-73.
[17] Tillner E, Langer M, Kempka T, Kühn M. Fault damage zone volume and initial salinity distribution determine intensity of shallow aquifer salinisation in subsurface storage. Hydrology and Earth System Sciences 2016; 20(3):1049-67.
[18] Vilarrasa V, Carrera J, Olivella S. Hydromechanical characterization of CO_2 injection sites. International Journal of Greenhouse Gas Control 2013; 19:665-77.
[19] Olivella S, Carrera J, Gens A, Alonso EE. Nonisothermal multiphase flow of brine and gas through saline media. Transport in Porous Media 1994; 15(3):271-93.
[20] Olivella S, Gens A, Carrera J, Alonso EE. Numerical formulation for a simulator (CODE_BRIGHT) for the coupled analysis of saline media. Engineering Computations 1996; 13(7):87-112.
[21] Vilarrasa V, Bolster D, Olivella S, Carrera J. Coupled hydromechanical modeling of CO_2 sequestration in deep saline aquifers. International Journal of Greenhouse Gas Control 2010; 4(6):910-9.
[22] Vilarrasa V, Silva O, Carrera J, Olivella S. Liquid CO_2 injection for geological storage in deep saline aquifers. International Journal of Greenhouse Gas Control 2013; 14:84-96.
[23] Bear J (ed.). *Dynamics of fluids in porous media*. Elsevier, New York, 1972.
[24] Vilarrasa V, Olivella S, Carrera J. Geomechanical stability of the caprock during CO_2 sequestration in deep saline aquifers. Energy Procedia 2011; 4:5306-13.
[25] Makhnenko RY, Labuz JF. Plane strain testing with passive restraint. Rock Mechanics Rock Engineering 2014; 47(6):2021-29.
[26] Makhnenko RY, Labuz JF. Elastic and inelastic deformation of fluid-saturated rock. Philosophycal Transactions of Royal Society A 2016; 374:20150422.
[27] Heuze F. Scale effects in the determination of rock mass strength and deformability. Rock Mechanics 1980; 12:167-92.
[28] Gräsle W. Multistep triaxial strength tests: investigating strength parameters and pore pressure effects on Opalinus clay. Physics and Chemistry of the Earth 2011; 36: 1898-1904.
[29] Labuz JF, Biolzi L. Characteristic strength of quasi-brittle materials. International Journal of Solids & Structures 1998; 35(31-32): 4191-203.
[30] Mylnikov D, Makhnenko RY, Vilarrasa V, Laloui L. Hydromechanical aspects of CO_2 breakthrough into clay-rich caprocks. Energy Procedia 2017 (this issue).
[31] Bennion B, Bachu S. Drainage and imbibition relative permeability relationships for supercritical CO_2/brine and H_2S/brine systems in intergranular sandstone, carbonate, shale, and anhydrite rocks. SPE Reservoir Evaluation & Engineering 2008; 11(03):487-96.
[32] Billi A, Salvini F, Storti F. The damage zone-fault core transition in carbonate rocks: implications for fault growth, structure and permeability. Journal of Structural Geology 2003; 25(11):1779-94.
[33] Egholm DL, Clausen OR, Sandiford M, Kristensen MB, Korstgård JA. The mechanics of clay smearing along faults. Geology 2008; 36(10):787-90.
[34] Rinaldi AP, Jeanne P, Rutqvist J, Cappa F, Guglielmi Y. Effects of fault-zone architecture on earthquake magnitude and gas leakage related to CO_2 injection in a multi-layered sedimentary system. Greenhouse Gases: Science and Technology 2014; 4(1):99-120.
[35] Makhnenko RY, Harvieux J, Labuz JF. Paul-Mohr-Coulomb failure surface of rock in the brittle regime. Geophysical Research Letters 2015; 42:6975-81.
[36] Kanamori H, Anderson DL. Theoretical basis of some empirical relations in seismology. Bulletin of the Seismological Society of America 1975; 65(5):1073-95.
[37] Stork AL, Verdon JP, Kendall JM. The microseismic response at the In Salah Carbon Capture and Storage (CCS) site. International Journal of Greenhouse Gas Control 2015; 32:159-71.
[38] Caine JS, Evans JP, Forster CB. Fault zone architecture and permeability structure. Geology 1996; 24(11):1025-8.
[39] Rutqvist J, Rinaldi AP, Cappa F, Jeanne P, Mazzoldi A, Urpi L, Guglielmi Y, Vilarrasa V. Fault activation and induced seismicity in geologic carbon storage - Lessons learned from recent modeling studies. Journal of Rock Mechanics and Geotechnical Engineering 2016; doi: 10.1016/j.jrmge.2016.09.001.
[40] Guglielmi Y, Cappa F, Avouac JP, Henry P, Elsworth D. Seismicity triggered by fluid injection–induced aseismic slip. Science 2015; 348(6240):1224-6.